

CrossMark  
click for updatesCite this: *Chem. Sci.*, 2016, 7, 5171

# Superior anion induced shuttling behaviour exhibited by a halogen bonding two station rotaxane†

Timothy A. Barendt, Sean W. Robinson and Paul D. Beer\*

Two bistable halogen and hydrogen bonding-naphthalene diimide [2]rotaxanes have been prepared and the system incorporating a halogen bond donor anion recognition site is demonstrated to exhibit superior anion induced translational motion of the macrocyclic wheel component relative to the hydrogen bonding analogue. Proton NMR spectroscopy is used to estimate the percentage occupancies of the macrocycle at the respective station and importantly indicates that the halogen bonding rotaxane displays superior positional integrity in competitive protic solvent media as a consequence of strong halogen bond–halide anion binding interactions.

Received 19th February 2016

Accepted 19th April 2016

DOI: 10.1039/c6sc00783j

www.rsc.org/chemicalscience

## Introduction

With the growing demand for smaller and more efficient computing devices, it has been proposed that the next wave of technology could use individual molecules as a way of rapidly handling vast amounts of data on the nanometre scale.<sup>1</sup> As a consequence, the controlling of molecular motion by using dynamic interlocked structures is receiving an increasing amount of interest.<sup>2–7</sup> This is motivated by the promise of their potential applications in nanotechnology as machines,<sup>7</sup> switches,<sup>4,7,8</sup> sensors<sup>9,10</sup> or delivery systems<sup>11–14</sup> where dynamic behaviour is driven by a variety of light-, chemical- and redox-based stimuli.<sup>4,7,15–18</sup> Whilst examples of cation binding-induced co-conformational change<sup>4,7</sup> within a rotaxane or catenane are prevalent in the literature, systems that use anions<sup>19–27</sup> as an external stimulus to produce molecular motion are relatively rare.

According to IUPAC “a halogen bond [XB] occurs when there is evidence of a net attractive interaction between an electrophilic region associated with a halogen atom in a molecular entity and a nucleophilic region in another, or the same, molecular entity”.<sup>28</sup> The integration of XB donor motifs into the scaffold of an anion receptor has resulted in contrasting and, in some cases, enhanced anion recognition behaviour in comparison to hydrogen bonding (HB) receptor analogues in protic organic solvent mixtures and recently in pure water.<sup>29–32</sup> This has also led to the development of the first interlocked structure utilising XB anion recognition to control translational molecular motion.<sup>33</sup>

Herein we report the syntheses of two novel cationic XB and HB bistable rotaxanes and demonstrate their capability to perform molecular shuttling upon changing the nature of the counter anion and the solvent. Both rotaxanes comprise of an isophthalamide-containing macrocycle threaded by a potential two station axle. The axle component contains an electron-deficient naphthalene diimide (NDI) motif capable of aromatic donor–acceptor charge-transfer interactions with the electron-rich hydroquinone groups of the macrocycle<sup>34,35</sup> and as the second station, an XB iodo- or HB proto-triazolium group capable of anion coordination. Molecular motion of the



Fig. 1 Schematic of the anion induced translational molecular motion within a bistable [2]rotaxane. NDI = naphthalene diimide, T<sup>+</sup> = triazolium, X = H (HB donor) or I (XB donor) and A<sup>−</sup> = Cl<sup>−</sup> or I<sup>−</sup>.

Chemistry Research Laboratory, Department of Chemistry, University of Oxford, 12, Mansfield Road, Oxford, OX1 3TA, UK. E-mail: paul.beer@chem.ox.ac.uk; Fax: +44 (0)1865 272690; Tel: +44 (0)1865 285142

† Electronic supplementary information (ESI) available. CCDC 1454515. For ESI and crystallographic data in CIF or other electronic format see DOI: 10.1039/c6sc00783j

macrocyclic wheel component from the NDI station to the triazolium group is demonstrated upon addition of a coordinating halide anion as the external stimulus (Fig. 1). Importantly, superior shuttling behaviour is exhibited by the XB rotaxane in competitive  $\text{CDCl}_3$  :  $\text{CD}_3\text{OD}$  solvent mixtures as a consequence of strong XB-halide anion binding.

## Results and discussion

### Synthesis of HB and XB two station rotaxanes

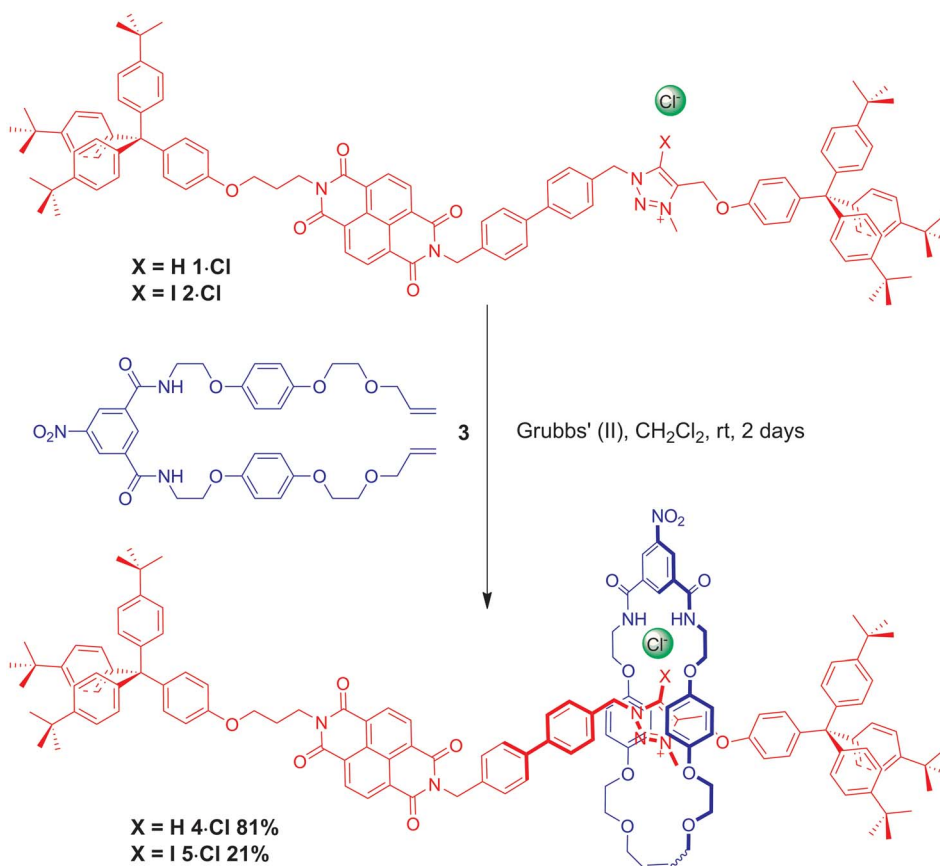
The HB and XB two station rotaxanes **4·Cl** and **5·Cl** were prepared by multistep synthetic pathways as described in the ESI†. Chloride anion-templation was used to facilitate ring closing metathesis (RCM) of a bis-vinyl-functionalised macrocyclic precursor **3** around the appropriate HB or XB asymmetric axle (**1·Cl** and **2·Cl** respectively) using Grubbs' II catalyst in dry dichloromethane. Preparative silica thin-layer chromatography purification afforded the desired rotaxanes (Scheme 1) which were characterised by  $^1\text{H}$ ,  $^{13}\text{C}$  and  $^1\text{H}$  2D ROESY NMR spectroscopy and by high resolution mass spectrometry (see ESI†).

### Investigations into anion-induced molecular motion

A comparison of the  $^1\text{H}$  NMR spectra of the axle components **1·Cl** and **2·Cl** with their respective rotaxanes **4·Cl** and **5·Cl**, in  $\text{CDCl}_3$ , was used to indicate the co-conformation of both

interlocked structures in the presence of the coordinating chloride anion (Fig. 2). Exclusive upfield shifts of the triazolium proton  $\text{H}_\text{m}$  (in the case of the HB rotaxane **4·Cl**), *N*-methyl triazolium group  $\text{H}_\text{l}$  and the alkyl groups ( $\text{H}_\text{k}$  and  $\text{H}_\text{n}$ ) either side of the triazolium station are observed on comparing the  $^1\text{H}$  NMR spectra of the axle and rotaxane. This is indicative of halide anion coordination by multiple HB and, in the case of **5·Cl**, XB, interactions within the unique three-dimensional cavity created between the axle and the macrocycle occupying the triazolium station. In contrast there is no change in the chemical shift of the NDI aromatic protons  $\text{H}_{\text{e,e'}}$  or its proximal alkyl protons  $\text{H}_\text{f}$  and  $\text{H}_\text{d}$  which suggests the macrocycle resides almost exclusively at the triazolium station in both rotaxanes. These co-conformations were confirmed by two-dimensional  $^1\text{H}$  ROESY NMR experiments in  $\text{CDCl}_3$  that showed, amongst other evidence, only cross coupling between hydroquinone protons of the macrocycle  $\text{H}_{\gamma,\gamma'}$  and triazolium *N*-methyl protons  $\text{H}_\text{l}$ , with no interaction between  $\text{H}_{\gamma,\gamma'}$  and the NDI protons  $\text{H}_{\text{e,e'}}$  (see ESI†).

Anion exchange to the corresponding hexafluorophosphate salts was achieved by repeatedly passing a solution of the rotaxane through a column containing an Amberlite® IRA-400 resin loaded with  $\text{PF}_6^-$ . A comparison of the resulting  $^1\text{H}$  NMR spectra of rotaxanes **4·PF<sub>6</sub>** and **5·PF<sub>6</sub>** with their respective chloride salts **4·Cl** and **5·Cl** in  $\text{CDCl}_3$  indicated a change in co-conformation had occurred as a result of shuttling of the



Scheme 1 Syntheses of HB and XB rotaxanes **4·Cl** and **5·Cl** by an anion-templated clipping methodology.



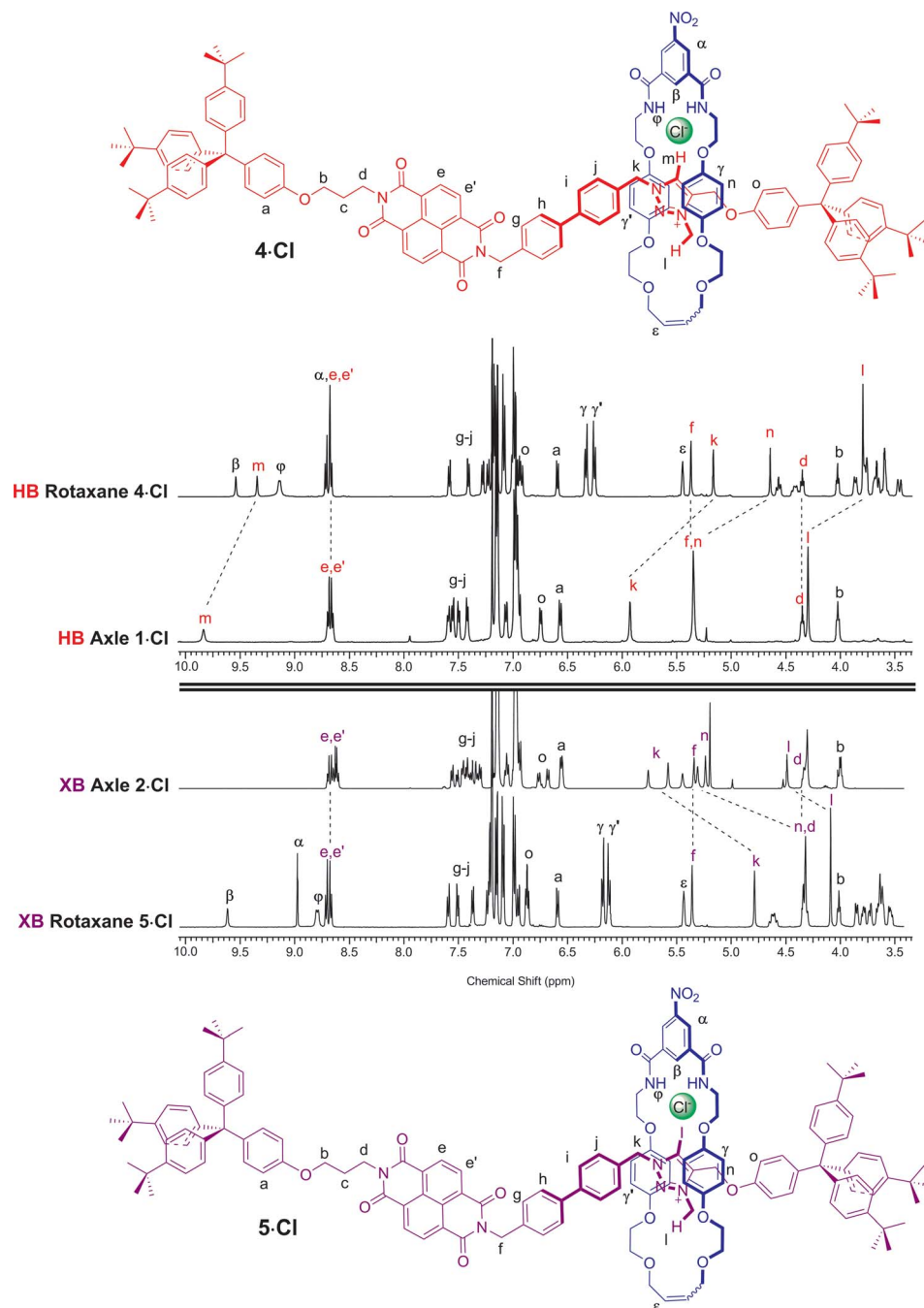


Fig. 2 Comparison of the truncated  $^1\text{H}$  NMR spectra ( $\text{CDCl}_3$ , 298 K, 400 MHz) of axles 1-Cl and 2-Cl and [2]rotaxanes 4-Cl and 5-Cl with their respective expected co-conformations.

macrocycle component to occupy the NDI station of the axle (Fig. 3). This is inferred by upfield shifts of the macrocycle hydroquinone protons  $\text{H}_{\gamma,\gamma'}$  which are indicative of stronger aromatic donor-acceptor charge-transfer interactions between the axle's electron-deficient NDI motif and macrocycle hydroquinone groups. In addition, upfield shifts of the NDI station protons  $\text{H}_{e,e'}$ , in contrast to a downfield shift of the *N*-methyl triazolium protons  $\text{H}_i$ , also suggests that shuttling of the macrocyclic component to the NDI station had taken place. Interestingly, the largest shifts are observed in the XB two station rotaxane 5- $\text{PF}_6$  indicating a greater degree of

translocation within this system has occurred than the HB analogue 4- $\text{PF}_6$ . The changes to the co-conformations are further evidenced by the  $^1\text{H}$  2D ROESY NMR spectra of 4- $\text{PF}_6$  and 5- $\text{PF}_6$ , both showing the appearance of new correlations between resonance signals arising from the macrocycle hydroquinone protons  $\text{H}_{\gamma,\gamma'}$  and the NDI protons  $\text{H}_{e,e'}$  (see ESI†).

Originally colourless as chloride salts 4-Cl and 5-Cl, donor-acceptor charge-transfer interactions between the macrocycle hydroquinone motifs and the extended  $\pi$  surface of the NDI station resulting from the shuttling behaviour upon conversion to rotaxanes 4- $\text{PF}_6$  and 5- $\text{PF}_6$  gave rise to a bright, distinctive





Fig. 3 Comparison of the truncated  $^1\text{H}$  NMR spectra ( $\text{CDCl}_3$ , 298 K, 400 MHz) of [2]rotaxanes **4**·Cl, **5**·Cl, **4**· $\text{PF}_6$  and **5**· $\text{PF}_6$  with their predicted co-conformations in the presence of  $\text{PF}_6^-$ .

orange colour (Fig. 4). Hence molecular motion can be detected by the naked eye through this colorimetric sensing response and was also demonstrated to be reversible using UV-vis spectroscopic studies (see ESI†).

#### X-ray crystallography<sup>36</sup>

Crystals suitable for X-ray diffraction structural analysis were obtained for the chloride salt of the XB rotaxane **5**·Cl by slow

evaporation of a solution of the rotaxane in 1 : 1  $\text{CDCl}_3$  :  $\text{CD}_3\text{OD}$ . The rotaxane crystallises in  $P\bar{1}$  where the asymmetric unit comprises the rotaxane as a 1 : 1 complex with chloride, as well as one molecule each of chloroform and water. Notably, the solid-state structure of the chloride salt of the XB rotaxane shows the macrocycle situated exclusively at the triazolium station, templated by the presence of the coordinating chloride anion ( $D_{\text{T} \cdots \text{Cl}^-} = 2.987(6)$  Å) (Fig. 5). This chloride anion  $\cdots$ iodo-







Fig. 4 Schematic of the anion-induced molecular shuttling exhibited by rotaxanes 4·A and 5·A and the colour of their two co-conformations in  $\text{CDCl}_3$  solution.



Fig. 5 X-ray crystal structure of 5·Cl showing the macrocycle (blue) situated at the iodo-triazolium station on the axle (red), templated by the coordinated chloride anion (green). Notable hydrogen and halogen bonding interactions are shown as dotted red lines with the atoms involved shown as spheres. Non-coordinating hydrogens and the co-crystallised chloroform and water molecules are omitted for clarity.

triazolium halogen bond is much shorter than the sum of the van der Waals radii (80%), indicating a very strong interaction. The structure is in agreement with the aforementioned  $^1\text{H}$  NMR evidence for the favoured co-conformation of the molecular shuttle in the presence of a coordinating anion.

### Effect of anion and solvent variation on percentage occupancies

In order to further investigate how the effect of varying the nature of the counter anion influenced the co-conformation of the XB and HB molecular shuttles, three new one-station rotaxanes containing either a proto-triazolium (6·Cl), iodo-triazolium (7·Cl) or NDI (8) motif were synthesised by multistep synthetic pathways and characterised by  $^1\text{H}$  and  $^{13}\text{C}$  NMR spectroscopy and by high resolution mass spectrometry as described in the ESI† (Fig. 6). These rotaxanes acted as models for the two station shuttles and enabled estimations of the station percentage occupancies by the macrocycle to be determined in the presence of non-coordinating  $\text{PF}_6^-$  and chloride and iodide anions.<sup>37</sup>

The  $^1\text{H}$  NMR spectra of these three rotaxanes in  $\text{CDCl}_3$  gave the proton chemical shift values of each station's diagnostic protons when there was complete occupancy by the macrocycle; specifically the *N*-methyl protons of the triazolium ring ( $\text{H}_i$ ) and those of the NDI aromatic protons ( $\text{H}_{e,e'}$ ). The chemical shift values for the same protons at 0% occupancy were obtained

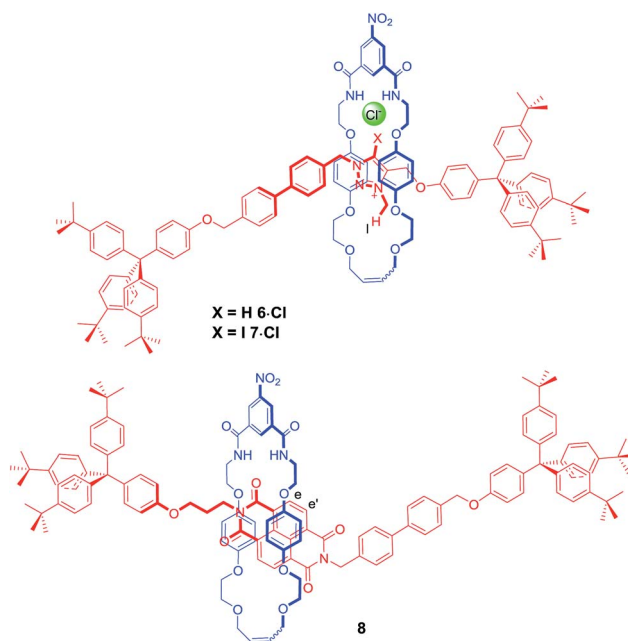


Fig. 6 The structures of the three model one station rotaxanes 6·Cl, 7·Cl and 8.

from the  $^1\text{H}$  NMR spectra in  $\text{CDCl}_3$  of the two-station axes 1·A and 2·A for a particular anion (A). Using these data, chemical shift scales were determined with respect to each station in the



presence of each anion, to characterise the two extremes of macrocycle occupation (see ESI†). This method was necessary because the dynamic behaviour of the bistable rotaxanes was fast on the  $^1\text{H}$  NMR timescale.

The complete occupation of the triazolium station by the macrocycle in the HB two station rotaxane system in the chloride salt (**4·Cl**) was confirmed by comparison of the chemical shift of the *N*-methyl triazolium protons in **4·Cl** ( $\delta(\text{H}_1) = 3.88$  ppm) with the  $\delta$  HB *N*-methyl triazolium chloride chemical shift scale. This was supported by an analogous comparison of the chemical shift of the NDI protons,  $\delta(\text{H}_{\text{e,e'}})$ , in **4·Cl** with the NDI chemical shift scale which indicated zero occupancy of the NDI station. This method was used to determine the macrocycle occupancies of both HB and XB rotaxane **4·A** and **5·A** halide

and  $\text{PF}_6^-$  salts using the appropriate *N*-methyl triazolium chemical shift scale (reported in Fig. 7) and concurred using the NDI chemical shift scale (see ESI†).

From these data it may be seen that both two-station rotaxanes exhibit anion induced molecular motion in  $\text{CDCl}_3$  solution (Fig. 7). The preference for the triazolium station in the chloride salts (**4·Cl** and **5·Cl**) was evident for both HB (100% occupancy of the triazolium station) and XB (92%) rotaxane switches, giving excellent positional integrity within this state. The same was true for the iodide salts (**4·I** and **5·I**), with the HB and XB rotaxanes estimated to have 100% and 95% occupancies of their triazolium stations respectively. Upon exchange to the non-coordinating  $\text{PF}_6^-$  salt, both systems demonstrated an increase in occupancy of the NDI station (Fig. 7), as expected from the

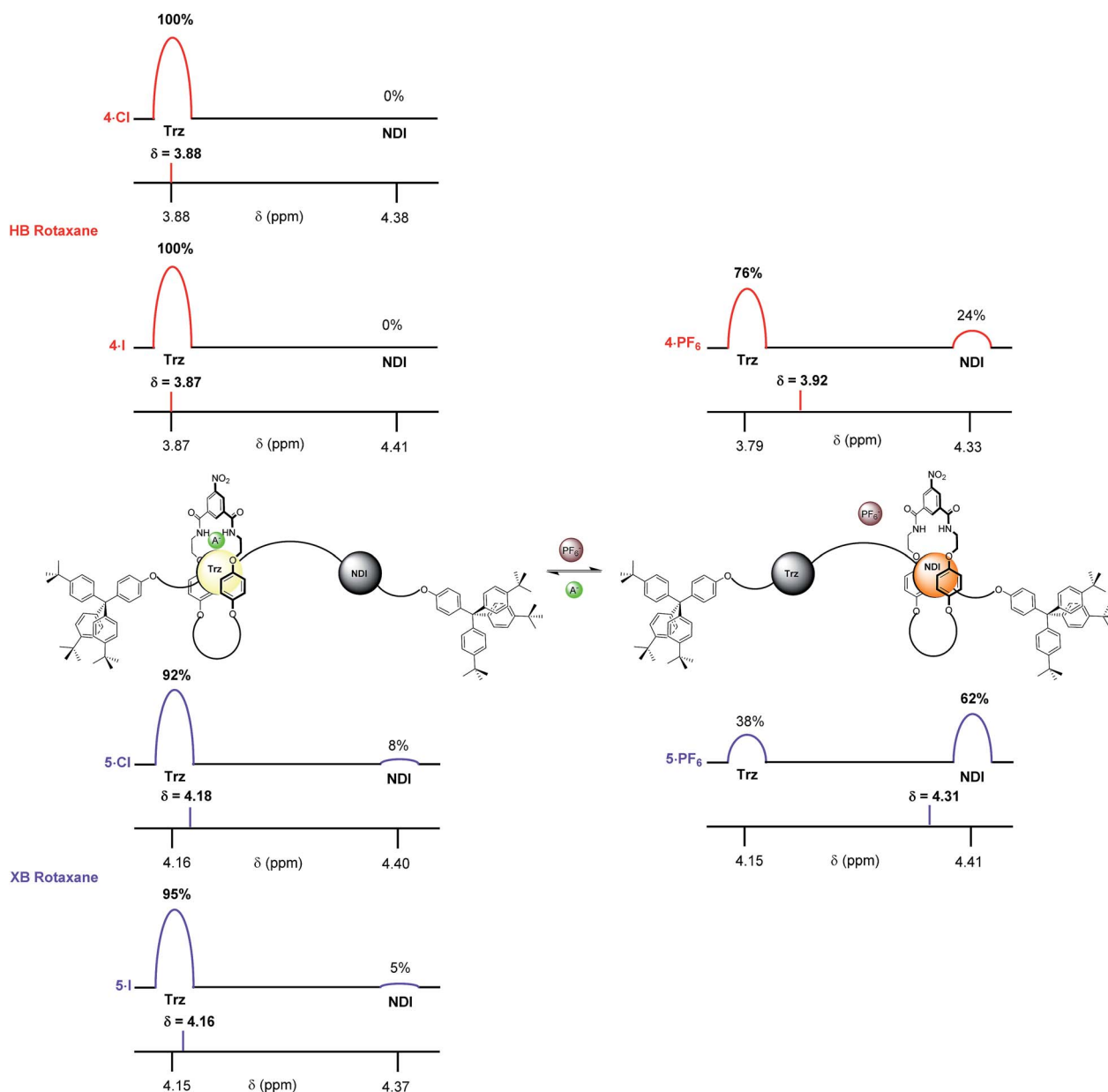


Fig. 7 The estimated percentage occupancies (based upon  $\text{H}_1$  protons) of the HB and XB rotaxanes **4·A** and **5·A** as chloride, iodide and  $\text{PF}_6^-$  salts as determined by  $^1\text{H}$  NMR spectroscopy in  $\text{CDCl}_3$  solution.  $\text{A}^- = \text{Cl}^-$  or  $\text{I}^-$  and Trz = triazolium.



one- and two-dimensional  $^1\text{H}$  NMR spectroscopy data discussed earlier. The largest occupation of the NDI station was found to occur with the XB rotaxane  $5 \cdot \text{PF}_6^-$  (62%) relative to the HB rotaxane  $4 \cdot \text{PF}_6^-$  (24%).<sup>38</sup> This indicated the XB rotaxane behaves as a superior molecular shuttle to the HB analogue on account of the larger swing in percentage occupancy of the stations upon anion exchange (>54% for the XB rotaxane vs. 24% for the HB rotaxane).

The propensity for anion receptors containing XB donor groups to exhibit enhanced halide, in particular iodide, anion recognition properties over their HB analogues in protic organic solvents<sup>30,31</sup> provided the impetus for investigating the shuttling behaviour in more competitive solvent mixtures. The percentage occupancies of the HB and XB rotaxane  $\text{PF}_6^-$ , chloride and iodide salt systems were estimated in competitive 4 : 1  $\text{CDCl}_3$  :  $\text{CD}_3\text{OD}$  and 1 : 1  $\text{CDCl}_3$  :  $\text{CD}_3\text{OD}$  solvent mixtures via analogous  $^1\text{H}$  NMR spectroscopic experiments monitoring

the chemical shifts of the respective rotaxane salt *N*-methyl triazolium  $\text{H}_1$  protons. Importantly, the results revealed a significantly enhanced positional integrity, in favour of the triazolium station for the XB rotaxane halide salt systems.

In 4 : 1  $\text{CDCl}_3$  :  $\text{CD}_3\text{OD}$  the difference in behaviour between XB and HB rotaxanes was most strongly manifested within the iodide salt of the rotaxanes. XB rotaxane  $5 \cdot \text{I}^-$  exhibited a 92% occupancy of the triazolium station whereas the HB analogue  $4 \cdot \text{I}^-$  was estimated at 70% (Fig. 8). The differences between the chloride salt occupancies of the triazolium stations of the two rotaxanes were, by contrast, smaller: XB rotaxane  $5 \cdot \text{Cl}^-$  was 100% vs. 87% for the HB rotaxane  $4 \cdot \text{Cl}^-$  (Fig. 8). This is a consequence of superior halide affinity afforded by strong XB formation from the rotaxane's iodo-triazolium anion recognition site in comparison to the weaker proto-triazolium HB donor motif in the competitive solvent medium. Upon exchange to their respective  $\text{PF}_6^-$  salts, an enhanced positional integrity in favour



Fig. 8 The estimated percentage occupancies (based upon  $\text{H}_1$  protons) of the HB and XB rotaxanes  $4 \cdot \text{A}^-$  and  $5 \cdot \text{A}^-$  as chloride, iodide and  $\text{PF}_6^-$  salts as determined by  $^1\text{H}$  NMR spectroscopy in 4 : 1  $\text{CDCl}_3$  :  $\text{CD}_3\text{OD}$  solution.  $\text{A}^- = \text{Cl}^-$  or  $\text{I}^-$  and Trz = triazolium.

of the NDI station was observed within the XB system  $5 \cdot \text{PF}_6$  (48% occupancy of the NDI station), relative to the HB rotaxane  $4 \cdot \text{PF}_6$  (33%), the same trend as found in  $\text{CDCl}_3$  solution.

Finally, the percentage occupancies of both XB and HB rotaxane iodide and  $\text{PF}_6^-$  salts were estimated in the more competitive solvent medium of 1 : 1  $\text{CDCl}_3$  :  $\text{CD}_3\text{OD}$  using  $^1\text{H}$  NMR spectroscopy experiments based upon the  $\text{H}_1$  protons (Fig. 9). The HB and XB rotaxanes were estimated to have the same occupancy of the NDI station as their  $\text{PF}_6^-$  salts (67%). However, a significantly larger preference for the triazolium station was exhibited in the iodide salt by the XB system  $5 \cdot \text{I}$  (63% occupancy of the triazolium station), over the HB system  $4 \cdot \text{I}$  (36%). This enabled the XB shuttle to still perform effectively in 1 : 1  $\text{CDCl}_3$  :  $\text{CD}_3\text{OD}$  and produce a significant percentage of

iodide induced molecular motion whereas the HB system afforded only negligible changes in the occupancies of the stations upon anion exchange. Analogous to previous solvent systems, there were smaller differences between occupancies of the triazolium stations in the chloride salts of HB and XB rotaxanes  $4 \cdot \text{Cl}$  and  $5 \cdot \text{Cl}$  (Fig. 9).

These experiments demonstrate that an enhanced positional integrity for the triazolium station in the halide state is achievable upon increasing the competitive nature of the solvent system, but only when it is facilitated by the XB interaction with iodide. As such, the XB rotaxane switch is demonstrated to be a superior example of a synthetic molecular shuttle over its HB analogue in both  $\text{CDCl}_3$  and competitive  $\text{CDCl}_3$  :  $\text{CD}_3\text{OD}$  solvent mixtures.



Fig. 9 The estimated percentage occupancies (based upon  $\text{H}_1$  protons) of the HB and XB rotaxanes  $4 \cdot \text{A}$  and  $5 \cdot \text{A}$  as iodide and  $\text{PF}_6^-$  salts as determined by  $^1\text{H}$  NMR spectroscopy in 1 : 1  $\text{CDCl}_3$  :  $\text{CD}_3\text{OD}$  solution.  $\text{A}^- = \text{Cl}^-$  or  $\text{I}^-$  and Trz = triazolium.



## Conclusions

In conclusion, the synthesis of five novel rotaxanes including two bistable rotaxanes and three model mono station systems are reported. Both cationic XB/HB two station rotaxanes were demonstrated to undergo halide anion induced molecular switching of their co-conformations in  $\text{CDCl}_3$  solution, with the added benefit that this shuttling behaviour resulted in a distinct colour change of the solution, giving a naked eye response to the translocation of the macrocyclic component. The XB two station rotaxane **5** demonstrated superior molecular shuttling in  $\text{CDCl}_3$  solution over the HB analogue rotaxane **4**. Upon increasing the competitive nature of the solvent mixture to 4 : 1 and 1 : 1  $\text{CDCl}_3$  :  $\text{CD}_3\text{OD}$ , the XB two station rotaxane again demonstrated superior molecular shuttling. This was driven by the XB interaction between iodide and the iodo-triazolium XB donor anion recognition site within the axle component. These results were reflected by determined estimations of the percentage occupancies of the stations using  $^1\text{H}$  NMR spectroscopy. This is the first example of using XB in concert with donor-acceptor charge-transfer interactions to exert significant control over solution phase molecular shuttling motion within an interlocked supramolecular system. Importantly this highlights the real and exciting potential XB has in the future design of dynamic interlocked mechanically bonded nano-technological switchable systems.

## Acknowledgements

T. A. B. would like to thank the EPSRC for a DTA studentship. S. W. R would like to thank the Clarendon Fund and St John's College, Oxford for funding. The authors would like to thank Dr Nicholas G. White (ANU) and Dr Amber L. Thompson (Oxford) for assistance with the crystallography as well as Diamond Light Source for an award of beamtime (MT9981).

## Notes and references

- 1 V. Balzani, A. Credi and M. Venturi, in *Molecular Devices and Machines – A Journey into the Nano World*, Wiley-VCH Verlag GmbH & Co. KGaA, 2003.
- 2 J. F. Stoddart, *Acc. Chem. Res.*, 2001, **34**, 410–411.
- 3 R. Ballardini, V. Balzani, A. Credi, M. T. Gandolfi and M. Venturi, *Acc. Chem. Res.*, 2001, **34**, 445–455.
- 4 E. R. Kay, D. A. Leigh and F. Zerbetto, *Angew. Chem., Int. Ed.*, 2007, **46**, 72–191.
- 5 A. Coskun, M. Banaszak, R. D. Astumian, J. F. Stoddart and B. A. Grzybowski, *Chem. Soc. Rev.*, 2011, **41**, 19–30.
- 6 E. A. Neal and S. M. Goldup, *Chem. Commun.*, 2014, **50**, 5128–5142.
- 7 S. Erbas-Cakmak, D. A. Leigh, C. T. McTernan and A. L. Nussbaumer, *Chem. Rev.*, 2015, **115**, 10081–10206.
- 8 K. Zhu, C. A. O'Keefe, V. N. Vukotic, R. W. Schurko and S. J. Loeb, *Nat. Chem.*, 2015, **7**, 514–519.
- 9 M. J. Chmielewski, J. J. Davis and P. D. Beer, *Org. Biomol. Chem.*, 2009, **7**, 415–424.
- 10 M. J. Langton and P. D. Beer, *Acc. Chem. Res.*, 2014, **47**, 1935–1949.
- 11 R. Klajn, J. F. Stoddart and B. A. Grzybowski, *Chem. Soc. Rev.*, 2010, **39**, 2203–2237.
- 12 V. Blanco, D. A. Leigh and V. Marcos, *Chem. Soc. Rev.*, 2015, **44**, 5341–5370.
- 13 M. Galli, J. E. M. Lewis and S. M. Goldup, *Angew. Chem., Int. Ed.*, 2015, **54**, 13545–13549.
- 14 S. Hoekman, M. O. Kitching, D. A. Leigh, M. Papmeyer and D. Roke, *J. Am. Chem. Soc.*, 2015, **137**, 7656–7659.
- 15 F. Vögtle, W. M. Müller, U. Müller, M. Bauer and K. Rissanen, *Angew. Chem., Int. Ed. Engl.*, 1993, **32**, 1295–1297.
- 16 V. Balzani, A. Credi and M. Venturi, *Chem. Soc. Rev.*, 2009, **38**, 1542–1550.
- 17 R. A. Bissell, E. Córdova, A. E. Kaifer and J. F. Stoddart, *Nature*, 1994, **369**, 133–137.
- 18 A. Livoreil, C. O. Dietrich-Buchecker and J.-P. Sauvage, *J. Am. Chem. Soc.*, 1994, **116**, 9399–9400.
- 19 J. Berná, C. Franco-Pujante and M. Alajarin, *Org. Biomol. Chem.*, 2013, **12**, 474–478.
- 20 G. T. Spence, M. B. Pitak and P. D. Beer, *Chem.–Eur. J.*, 2012, **18**, 7100–7108.
- 21 N. H. Evans, C. J. Serpell and P. D. Beer, *Chem.–Eur. J.*, 2011, **17**, 7734–7738.
- 22 C. J. Serpell, R. Chall, A. L. Thompson and P. D. Beer, *Dalton Trans.*, 2011, **40**, 12052–12055.
- 23 E. V. Dzyuba, L. Kaufmann, N. L. Löw, A. K. Meyer, H. D. F. Winkler, K. Rissanen and C. A. Schalley, *Org. Lett.*, 2011, **13**, 4838–4841.
- 24 J. J. Gassensmith, S. Matthys, J.-J. Lee, A. Wojcik, P. V. Kamat and B. D. Smith, *Chem.–Eur. J.*, 2010, **16**, 2916–2921.
- 25 H. Zheng, W. Zhou, J. Lv, X. Yin, Y. Li, H. Liu and Y. Li, *Chem.–Eur. J.*, 2009, **15**, 13253–13262.
- 26 T.-C. Lin, C.-C. Lai and S.-H. Chiu, *Org. Lett.*, 2009, **11**, 613–616.
- 27 M. J. Barrell, D. A. Leigh, P. J. Lusby and A. M. Z. Slawin, *Angew. Chem., Int. Ed.*, 2008, **47**, 8036–8039.
- 28 G. R. Desiraju, P. S. Ho, L. Kloo, A. C. Legon, R. Marquardt, P. Metrangolo, P. Politzer, G. Resnati and K. Rissanen, *Pure Appl. Chem.*, 2013, **85**, 1711–1713.
- 29 T. M. Beale, M. G. Chudzinski, M. G. Sarwar and M. S. Taylor, *Chem. Soc. Rev.*, 2013, **42**, 1667–1680.
- 30 L. C. Gilday, S. W. Robinson, T. A. Barendt, M. J. Langton, B. R. Mullaney and P. D. Beer, *Chem. Rev.*, 2015, **115**, 7118–7195.
- 31 M. J. Langton, S. W. Robinson, I. Marques, V. Félix and P. D. Beer, *Nat. Chem.*, 2014, **6**, 1039–1043.
- 32 G. Cavallo, P. Metrangolo, R. Milani, T. Pilati, A. Priimagi, G. Resnati and G. Terraneo, *Chem. Rev.*, 2016, **116**, 2478–2601.
- 33 A. Caballero, L. Swan, F. Zapata and P. D. Beer, *Angew. Chem., Int. Ed.*, 2014, **53**, 11854–11858.
- 34 L. Raehm, D. G. Hamilton and J. K. Sanders, *Synlett*, 2002, **2002**, 1743–1761.
- 35 G. Kaiser, T. Jarroson, S. Otto, Y.-F. Ng, A. D. Bond and J. K. M. Sanders, *Angew. Chem., Int. Ed.*, 2004, **43**, 1959–1962.



- 36 Single crystal X-ray diffraction data for the rotaxane structure were collected using synchrotron radiation at Diamond Lightsource (H. Nowell, S. A. Barnett, K. E. Christensen, S. J. Teat and D. R. Allan, *J. Synchrotron Radiat.*, 2012, **19**, 435). Raw frame data (including data reduction, inter-frame scaling, unit cell refinement and absorption corrections) were processed using CrysAlis Pro (Agilent Technologies, 2010). Structures were solved using SUPERFLIP (L. Palatinus and G. Chapuis, *J. Appl. Crystallogr.*, 2007, **40**, 786) and refined using CRYSTALS (P. W. Betteridge, J. R. Carruthers, R. I. Cooper, K. Prout and D. J. Watkin, *J. Appl. Crystallogr.*, 2003, **36**, 1487; R. I. Cooper, A. L. Thompson and D. J. Watkin, *J. Appl. Crystallogr.*, 2010, **43**, 1100; P. Parois, R. I. Cooper and A. L. Thompson, *Chem. Cent. J.*, 2015, **9**, 30). For further details of all crystallography, see the ESI.†
- 37 The rotaxanes were demonstrated to be excellent models of the two-station rotaxanes because the chemical shifts of the diagnostic protons for each station, that is the *N*-methyl protons of the triazolium chloride groups H<sub>1</sub> and the NDI aromatic protons H<sub>e,e'</sub>, of the model one station axes were identical to those found in the <sup>1</sup>H NMR spectra for the HB and XB two-station axes **1**·Cl and **2**·Cl.
- 38 The difference in behaviour of **4**·PF<sub>6</sub> and **5**·PF<sub>6</sub> under these conditions is not clear at present, however, we tentatively ascribe the lower occupancy of the iodo-triazolium station to potential steric repulsion between the macrocycle and the large iodine atom.

